



**COMPUMAG  
2009**



Florianópolis, Brazil

Proceedings of the  
**17<sup>th</sup> Conference on the Computation of  
Electromagnetic Fields**

November, 22<sup>nd</sup> – 26<sup>th</sup>  
Florianópolis, Brazil

ORGANISATION:



SPONSORING:



<b>PD1.12</b> .....	923
Improvement in accuracy of thermal FEM model partition wall with the use of optimization algorithm	
<i>Peter Kitak, Igor Ticar, Joze Pihler, Oszkar Biro, Kurt Preis</i>	
<b>PD1.13</b> .....	925
Field Computation and Performance of a Series-Connected Self-Excited Synchronous Generator	
<i>Tze-Fun Chan, Weimin Wang, Loi Lei Lai</i>	
<b>PD1.14</b> .....	927
Power Factor Calculation by the Finite Element Method	
<i>Claudia Andréa da Silva, Francis Bidaud, Philippe Herbet, José Roberto Cardoso</i>	
<b>PD1.15</b> .....	929
Comprehensive Research on Stator Shapes and Frames in Switched Reluctance Motor: Electromagnetic, Thermal and Vibration Analyses	
<i>Jian Li, Xueguan Song, Dawoon Choi, Yunhyun Cho</i>	
<b>PD1.16</b> .....	931
Investigation of System Efficiency in Nd-Fe-B and Ferrite Magnet Synchronous Motors with Coupled Field-Circuit Analysis	
<i>Tao Sun, Soon-O Kwon, Jung-Pyo Hong</i>	
<b>PD1.17</b> .....	933
Minimizing Torque Ripple of a BLDC Motor by Offsetting Cogging Torque with Voltage Control	
<i>Jin seok Jang, Byung teak Kim</i>	
<b>PD1.18</b> .....	935
A novel transverse flux linear motor for direct drive applications	
<i>Junghwan Chang, Jiwon Kim, Dohyun Kang, Deokje Bang</i>	
<b>PD1.19</b> .....	937
Design Strategy of Interior Permanent Magnet Synchronous Motor for Electric Power Steering Considering Cogging Torque and Torque Ripple using Current Harmonics	
<i>Soon-O Kwon, Jeong-Jong Lee, Tao Sun, Young-Kyun Kim, Geon-Ho Lee, Jung-Pyo Hong</i>	
<b>PD1.20</b> .....	939
Calculate the Parameters of IPMSM according to distance of PM and Magnetic saturation.	
<i>Ik Sang Jang, Chang Sung Jin, Seung Joo Kim, Ju Lee</i>	

# Investigation of System Efficiency in Nd-Fe-B and Ferrite Magnet Synchronous Motors with Coupled Field-Circuit Analysis

Tao Sun<sup>1</sup>, Soon-O Kwon<sup>1</sup>, Geun-Ho Lee<sup>1</sup>, Jin Hur<sup>2</sup> and Jung-Pyo Hong<sup>1</sup>, *Senior Member, IEEE*

Department of Automotive Engineering, Hanyang University, Seoul, CO 133791, Korea  
School of Electric Engineering, University of Ulsan, Ulsan, CO 5680749, Korea

This paper studies the influence of permanent magnet (PM) on the total motor system efficiency. Two PM synchronous motors with different magnets, same back electromotive force and same output power have been designed. An indirect coupled field-circuit method is used in this paper to calculate motor losses and inverter losses. First, a dynamic simulation is performed with the parameters of the semiconductor devices and these two motors. The current waveforms and inverter losses can be evaluated in this process. And then, using the current waveforms, and data of Epstein Frame method, the iron losses of these two motors will be calculated in a finite element method. The sum of the inverter losses, copper losses, and iron losses can be compared to reflect the influence of the magnet on the total system efficiency. Finally, the analysis results will be verified by the experiment.

*Index Terms*—coupled field-circuit analysis, ferrite, iron losses, neodymium, permanent magnet synchronous motor

## I. INTRODUCTION

FERRITE and Nd-Fe-B (Nd) magnets have been widely used in permanent magnet synchronous motors (PMSM) for a few decades. The ferrites, as known, are produced by powder metallurgy. The remanent flux densities of ferrite magnets usually are under 0.5T and the relative high operating temperature and low cost are their advantages. The Nd magnet is a type of rare-earth magnet. It is made from an alloy of neodymium, iron, and boron to form the  $\text{Nd}_2\text{Fe}_{14}\text{B}$  tetragonal crystalline structure. According to manufacture techniques, the Nd magnets are classified to Sintered type and Bonded type. The remanent flux density of Sintered type Nd magnet can achieve maximum 1.4 T. [1] Therefore, for the PMSM, the high power density can be easily achieved by using Nd magnet. One of the drawbacks of Nd magnet is the great cost due to the rare-earth component. Therefore, there is a compromise issue between the performance and cost when design the PMSM using ferrite or Nd magnets.

As the same back electromotive force (Back-EMF) and output power, the motor with ferrite magnet (ferrite motor) may have higher inductance than the one with Nd magnet (Nd motor) because of its more winding turns. The different inductance may lead to the different time constant which affects the switching efficiency of the motor drive and current waveforms. Additionally, the different current waveforms may produce different iron losses of motors. In order to investigate this conjecture about the influence of magnet on the motor system efficiency, an indirect coupled field-circuit method is employed in this paper. In the evaluation of switching losses, a dynamic simulation considering PWM current regulation is processed with the parameters of the inverter and these two motors. Using the obtained flowing current of IGBT, freewhe-

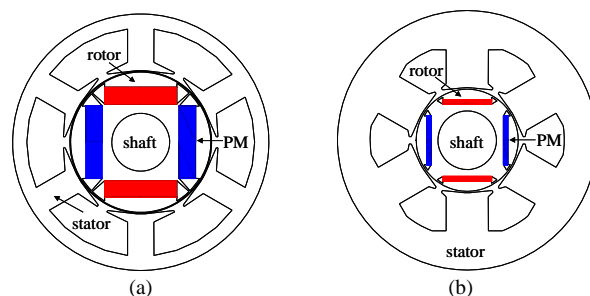


Fig. 1 Cross-section of analysis models: (a) ferrite motor; (b) Nd motor.

eling current of diode, and other inherent parameters, the switching losses can be estimated [2] and [3]. And then, depending on the data of Epstein Frame method and a finite element method (FEM), the iron losses of the motors can be calculated [8]. Finally, the influence of the magnet on the total system efficiency can be reflected by comparing the total losses of these two motors. The analysis result will be helpful to the determination of permanent magnet in the PMSM design.

## II. ANALYSIS MOTOR MODELS

Two PMSMs with ferrite and Nd magnets have been design for using in refrigerator compressor. The cross-section and specifications of these two motor models can be seen in Fig. 1 and Table I. In Fig. 2, the torque, output power, line-to-line voltage and line current of these two motors are compared in the total operation range. It is observed that the two motors are almost same in the characteristics.

Due to the low remanent flux density of ferrite magnet, the ferrite motor should have more turns of coil per phase in order to generate similar Back-EMF to Nd motor. The more turns of coil per phase, hence, result into higher inductance. The d- and q-axis inductances of these two motors are compared in Table

## III. INDIRECT COUPLED FIELD-CIRCUIT METHOD

In order to investigate the influence of PM on the total

Manuscript received December 23, 2009

Corresponding author: Jung-Pyo Hong (e-mail: hongjp@hanyang.ac.kr)

Digital Object Identifier inserted by IEEE

system efficiency, two domains: circuit and magnetic field

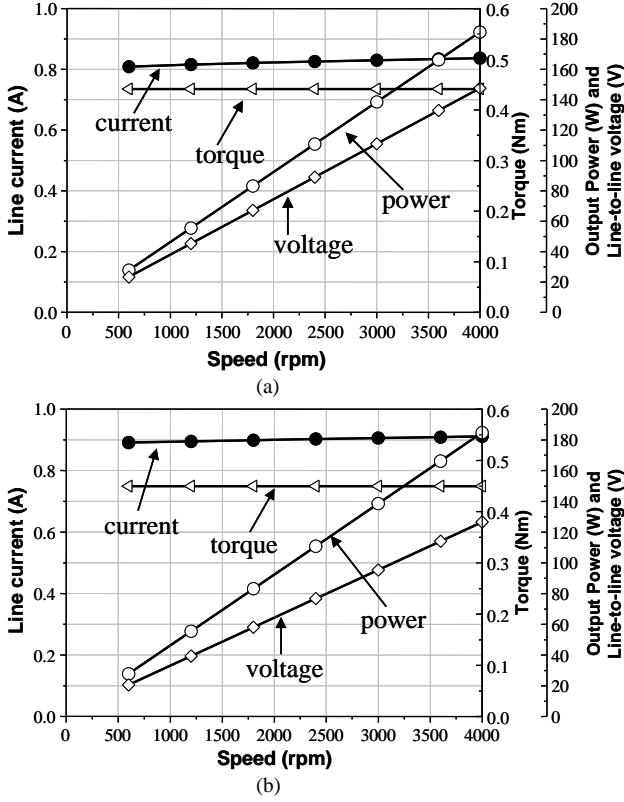


Fig. 2 Comparison of characteristics: (a) ferrite motor; (b) Nd motor.

should be calculated. The coupled field-circuit analysis method is satisfied to this case. The coupled field-circuit method includes direct method and indirect method. In the direct coupled field-circuit method, the equations of circuit domain and field domain are built into one simultaneous matrix and solved, while the equations of the two domains are built and solved independently in the indirect method. Although the direct method has higher precision than the indirect, its computation time also is much longer [5] and [6]. In this paper, the indirect coupled field-circuit will be used.

#### A. Modeling in Magnetic Field Domain

In the proposed indirect coupled field-circuit method, the 2D magneto-static field FEM is used in 2 calculation step:

Step 1: calculating the motor inductances; [4]

Step 2: calculating the magnetic field distribution with the known current waveforms and spatial steps.

The governing equation of the magnetostatic field FEM for PMSM, i.e. the nonlinear Poisson equation, is described in (1).

$$\nabla \times v(\nabla \times \mathbf{A}) = \mathbf{J} + \nabla \times (v\mu_0 \mathbf{M}) \quad (1)$$

where  $\mathbf{A}$  is the magnetic potential vector,  $\mathbf{J}$  is the current density vector,  $\mathbf{M}$  is the magnetization vector,  $v$  is the reluctivity, and  $\mu_0$  is the permeability of air.

#### B. Modeling in Circuit Domain

##### 1) Modeling of motor

According to the Park's transformation, the modeling equations of the PMSM can be described as (2)-(3). [4]

$$\begin{bmatrix} v_d \\ v_q \end{bmatrix} = \begin{bmatrix} R_a + pL_d & -\omega L_q \\ \omega L_d & R_a + pL_q \end{bmatrix} \begin{bmatrix} i_d \\ i_q \end{bmatrix} + \begin{bmatrix} 0 \\ \omega \psi_a \end{bmatrix} \quad (2)$$

$$T = \frac{3}{2} P [\psi_a i_q + (L_d - L_q) i_d i_q] \quad (3)$$

where  $R_a$  is the phase winding resistance,  $P$  is the number of pole pair,  $\omega$  is the electrical angular velocity, and  $\psi_a$  is the flux linkage of permanent magnet.

##### 2) Modeling of Inverter

In order to considering the PWM current regulation influence, the modeling of the voltage source inverter and PWM are necessary. The voltage source inverter is modeled by using of the switch function concept which is introduced in [7]. The pole voltage of phase a can be calculated by the following switching functions (4).

$$v_{ao} = \frac{V_{DC}}{2} \times (SF_{A\_top} - SF_{A\_bottom}) \quad (4)$$

where  $V_{DC}$  is the DC link voltage, and  $SF_x$  is the switching function of top and bottom switches. And, SF is 1 or 0 when the gate is on or off. After obtaining the all 3-phase pole voltages, the phase voltages can be expressed by the pole voltages as (5).

$$V_{an} = V_{ao} - \frac{V_{ao} + V_{bo} + V_{co}}{3} \quad (5)$$

In addition, a current vector controller also is considered in the modeling of circuit domain. In this paper, the ferrite motor is controlled at  $15^\circ$  current vector angle, while the Nd motor has  $6^\circ$  current vector angle in order to get maximum torque.

#### IV. LOSSES CALCULATION METHODS

##### A. Iron Losses Calculation Method

The dominant losses in PMSM usually consist of copper loss, iron losses and mechanical losses. The copper loss is determined by winding resistance which is constant in a given temperature. The mechanical losses can be calculated by a function of proportion with speed [4]. In this paper, a method which was proposed and verified in [9] is used to calculate the iron losses. It is described in Figure 3.

##### B. Switching Losses Calculation Method

As the transistors in switching-on or switching-off states, four kinds of losses are produced [2]. They are current conduction losses and switching losses in transistors and freewheeling diodes, respectively. Based on [2] and [3], the simplified calculation equations of these four losses are shown in (6)-(7).

$$P_{con} = \frac{1}{T} \int_0^T [(v_0 + r_0 \cdot i(t)^a) \cdot i(t)] dt \quad (6)$$

$$E_{sw} = b \cdot i(t)^c \quad (7)$$

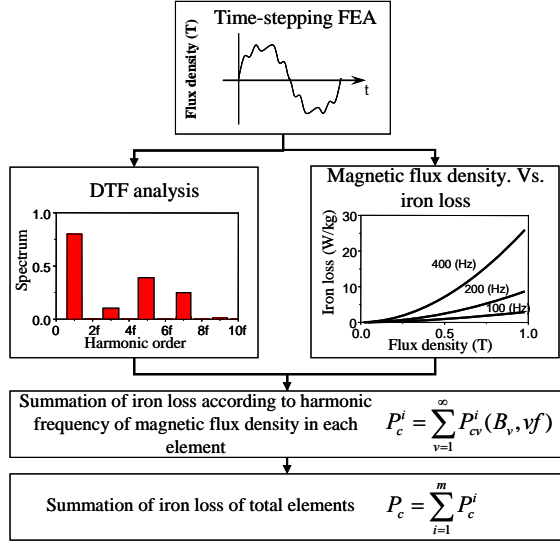


Fig. 3 Iron losses calculation process

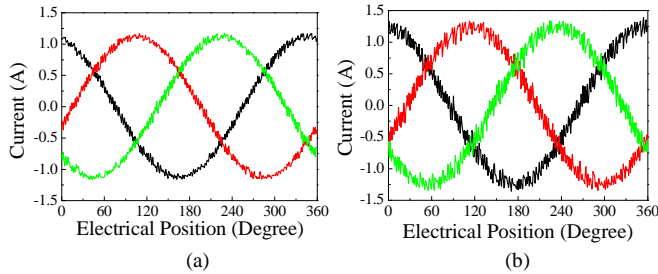


Fig. 4 Current waveform in 3000 Hz PWM: (a) current of ferrite motor; (b) current of Nd motor

where  $P_{con}$  is used to calculate the conduction losses of transistor and diode,  $E_{sw}$  is used to calculate the switching losses of transistor and diode,  $T$  is the fundamental period of current,  $v_0$  is the bias voltage for device,  $r_0$  is the resistance of device,  $i(t)$  is the transient current, and  $a$ ,  $b$ , and  $c$  are the curve fitted constant according to the datasheet of device. In this paper, the analysis inverter is the model FSBF5CH60B, product of Fairchild Company [9].

## V. ANALYSIS RESULTS AND DISCUSSIONS

The current waveforms of the two analysis motors calculated in the model of circuit domain are shown in Fig. 4. The load torque is 0.44 Nm, the operating speed is 3000 rpm. In the Fig. 4, the current waveforms of the two motors driven by the 3000 Hz PWM are compared. It is obvious that the current waveform of the ferrite magnet is smoother than that of the Nd motor, which verified the conjecture mentioned previously. In order to obtain the similar current waveform, the PWM frequency of Nd motor is increased to 6000 Hz. The statistic results of the inverter losses as different speed and PWM frequency are shown in Fig. 5. For the more smooth current waveforms, the Nd motor sacrifices the inverter efficiency.

Using the current waveforms obtained from the circuit domain, the iron losses are analyzed in 2D magneto-static FEM. Not only the PWM current waveforms, but also the ideal sinusoidal current waveforms are used to solve the magneto-static FEM. The iron losses of these two motors solved by sinusoidal and PWM current waveforms are compared in Fig. 6. In addition, the copper loss and mechanical loss as the same operation condition are calculated and shown in Fig. 7. Due to a little higher current, the Nd motor has higher copper loss, which also causes the larger inverter losses as shown in Fig. 5. A large difference occurs between the mechanical losses of the two motors. This is because the much greater radii and mass of the rotor of the ferrite motor increases the friction and area of windage.

The total system losses and efficiency are compared in Fig. 8. It can be seen that the Nd motor has higher efficiency in the total operation range. However, this predominance to the motor with ferrite magnet will be unregarded as the speed decreases. There is a great difference on the rotor structure so that the mechanical losses become dominant.

In order to verify the analysis methods of this paper, these two ferrite and Nd motors are manufactured and tested. The measured inverter losses and motor losses are shown in Fig. 9. As estimated in analysis results, the inverter of Nd motor consumes more losses due to its larger current. It also can be seen that the Nd motor has lower total losses. According to the analysis, the dominant reason of this difference is because of the mechanical losses. Therefore, as speed increases, the losses of ferrite motor increase more, and its total system efficiency becomes lower at high speed region.

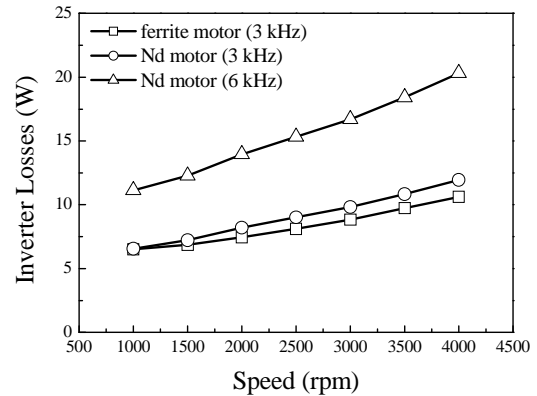


Fig. 5 Calculated inverter losses as variation of speed and PWM frequency

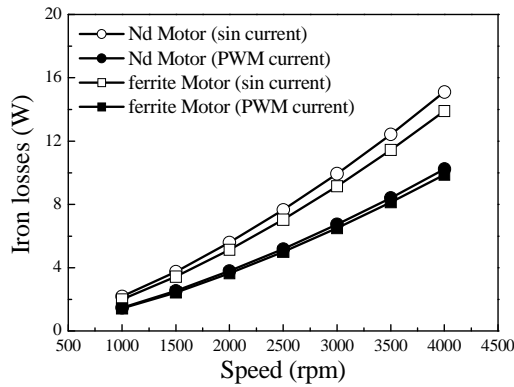


Fig. 6 Calculated iron losses as variation of speed in sine current waveform and PWM current waveform

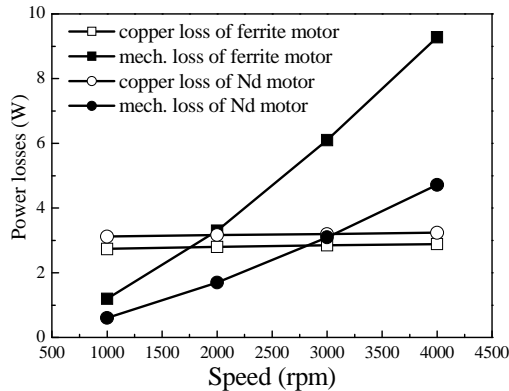


Fig.7 Comparisons of estimated copper loss and mechanical losses

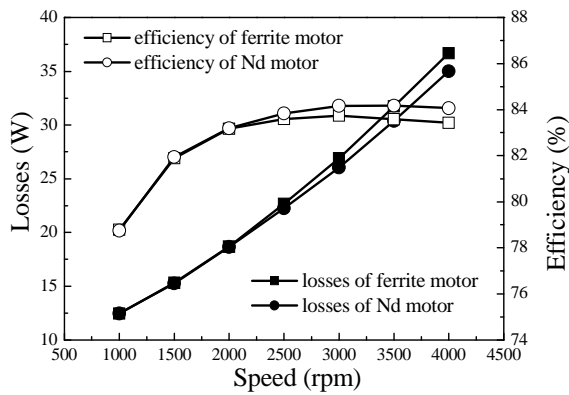


Fig. 8 Comparisons of estimated losses and efficiency of total motor system

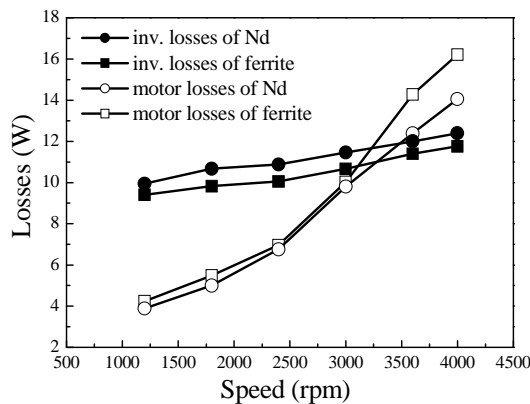


Fig. 9 Comparisons of measured losses of inverters and motors

## VI. CONCLUSION

This paper investigates the influence of PM on the total PMSM system efficiency. Two motors with different magnet and same output power are compared. By using an indirect coupled field-circuit method, the inverter losses, and iron losses of PMSM are calculated. As shown in results, due to the higher inductance, the ferrite motor generates lower iron losses in the PWM current exciting. Although the total efficiency of the ferrite motor is lower than the Nd motor due to the great mechanical losses, considering great magnet cost, there is a compromise between the using of Nd-Fe-B and ferrite magnets. As the same PWM frequency, ferrite motor behaves better

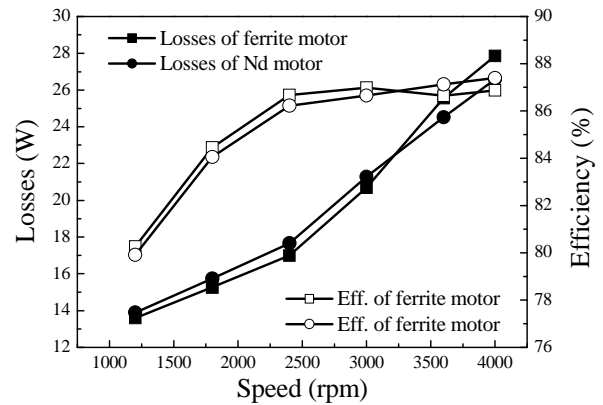


Fig. 10 Comparisons of measured losses and efficiency of two motor systems

performance at low speed operation region. Due to its larger radii and mass of rotor, low speed and high torque application case may be preferred to used the ferrite magnet. In addition, the noise and vibration of motor also will be affected by the current waveform. This issue will be analyzed in the further works.

TABLE I  
SPECIFICATION OF ANALYSIS MOTORS

Parameter	Ferrite motor	Nd motor
Inner radii of rotor	65 mm	45 mm
Air-gap/Stack length	0.7 mm / 45 mm	
Volume of magnet	$7.5 \times 33 \times 45 \text{ mm}^3$	$2 \times 22 \times 45 \text{ mm}^3$
Remanent flux density	0.46 T	1.3 T
No. of turns per phase	310	196
d-/q-axis inductance	32.57 / 72.54 mH	16.72 / 26.21 mH

## REFERENCES

- [1] Rollin. J. Parker, *Advances in Permanent Magnetism*, A Wiley-Interscience Publication, 1990, pp. 61-100.
- [2] F. Blaabjerg, U. Jaeger, S. Munk-Nielsen, "Power losses in PWM-VSI inverter using NPT or PT IGBT devices," *IEEE Trans. Power Electron.*, Vol. 10, No. 3, pp. 358-367, May 1995.
- [3] ANIP9931E, Calculation of Major IGBT Operating Parameters, Infineon technologies, www.infineon.com, Aug. 1999.
- [4] Tao. Sun, J. P. Hong, etc., "Determination of Parameters of Motor Simulation Module Employed in ADVISOR," *IEEE Trans. Magn.*, Vol. 44, No. 6, pp.1578-1581, June 2008.
- [5] L. Xu, and Ruckstadter E, "Direct modeling of switched reluctance machine by coupled field-circuit method," *IEEE Trans. Energy Convers.*, Vol. 10, No. 3, pp.446-454, Sept. 1995.

- [6] J. Y. Lee, G. H. Lee, J. P. Hong, J. Hur, "Coupled field circuit analysis for characteristic comparison in barrier type switched reluctance motor," *KIEE International Transactions on Electrical Machinery and Energy Conversion Systems.*, Vol. 5-B, No. 3, pp.267-271, 2005.
- [7] W. T. Lee, J. P. Hong, etc., "Object oriented modeling of an Interior Permanent Magnet Synchronous Motor Drives for Dynamic Simulation of Vehicular Propulsion," *IEEE Vehicle Power and Propulsion Conference, VPPC '06*, Sept. 2006.
- [8] J. J. Lee, J. P. Hong, etc., "Loss distribution of three phase induction motor fed by pulsewidth-modulated inverter," *IEEE Trans. Magn.*, Vol. 40, No. 2, pp.761-765, March 2004.
- [9] Application Note of FSBF5CH60B by Fairchild Company, [www.fairchildsemi.com](http://www.fairchildsemi.com)